

## Mechanical Characterization of Chitosan - A Marine Based Biomaterial

Juma, D. Hanif<sup>1</sup>, Katana G. Gabriel<sup>1</sup>, Agumba John<sup>1</sup>, Abdhalla Merenga<sup>2</sup> Tanui P. Kiprotich<sup>3</sup>

<sup>1</sup>Department of Physics, Pwani University, **Kilifi, (KENYA)**

<sup>2</sup>Department of Physics, Kenyatta University, **Nairobi, (KENYA)**

<sup>3</sup>Department of Physics, University of Eldoret, **Eldoret, (KENYA)**

### Abstract

In this study, mechanical properties of chitosan thin films extracted from the squid gladius found along the coastal areas of Kilifi and Mombasa in Kenya were investigated. Chitosan thin films were prepared by the solution cast technique. DMA analysis showed two dynamic processes; the beta relaxation process which generally seemed to increase with frequency and chitosan concentration and the alpha relaxation process or glass transition ( $T_g$ ). The temperature at which these two transitions occur gave an insight of the operating temperature range of the biomaterial. Arrhenius plots gave the activation energy of the biomaterial at ca.259kJ/mol which increased with chitosan concentration. Structural characteristics of the sample were discussed on the basis of the DMA analysis data.

**Key Words:** *Tapping mode AFM; Chitin Deacetylation; Biomaterial; Cantilever.*

### 1. Introduction

Recently, there has been an increasing interest in marine-derived polymers that are naturally biodegradable. The unique three dimensional, nano-organized scaffoldings of such polymers can yield desirable macro-physical attributes related to their mechanics, chemistry, and thermostability. Progress in soft condensed matter surfaces at the molecular level is today forming the building blocks for the creation of the next generation materials and devices in practically all scientific areas. In recent years, significant development has been achieved in biomaterials for various bioelectronics and biomedical applications. In particular, there is huge interest for biomedical applications. If properly investigated and implemented, marine -derived biomaterials are promising materials in various fields of electronics [1,2].

The study of thin film has greatly broadened the study of biomaterials by giving a clear indication of their chemical and physical properties. They have mechanical, electrical, magnetic and optical properties which differ from those of the bulk material. Currently, changes in the needs for thin film materials and devices are creating new opportunities for the development of new processes, materials and technologies. Knowledge of the physical, chemical and optical properties of any biomaterial thin films has to be established correctly in order to assign it to a given application. In particular, optical properties are directly related to structural and electronic properties of materials, and hence very important in device applications. Such knowledge provides a huge amount of information about their structure, optoelectronic behavior and transport of charge carriers [3,4].

Chitosan is a polysaccharide derived from naturally occurring chitin which is largely found in marine invertebrates, insects, fungi and yeast [5]. Pure chitin is completely acetylated; when deacetylated, its derivative is known as chitosan. The molecular structure of chitin, chitosan and cellulose is shown in Figure 1. There is no set definition in the literature for the acetylation/deacetylation cut-off between chitin and chitosan but it is generally accepted that chitin must be at least 30–40% acetylated, though natural samples are typically 85–95% acetylated [6]. Chitosan has emerged as a promising material for biological functionalization of microelectromechanical systems (MEMS) due to its unique chemical properties and film forming ability. It serves as a matrix for the assembly of biomolecules, cells, nanoparticles and other systems for life science applications.

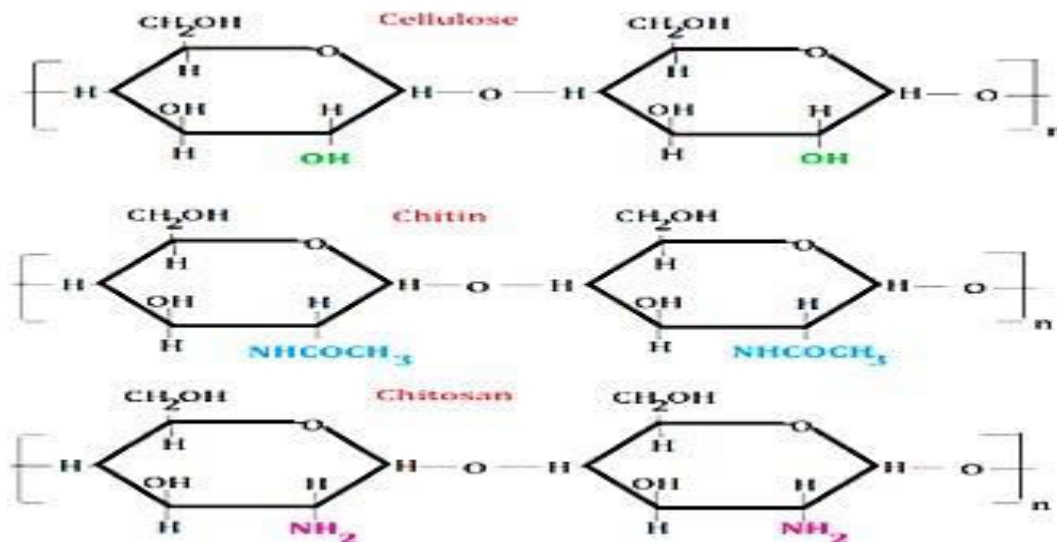


**Figure 1: Structure of cellulose, chitin and its chitosan**

Studies have demonstrated that the different geographical sources and species of chitosan are able to alter the functional properties of resulting chitin and chitosan [7, 8]. In Coastal Kenya and in particular Kilifi County, marine solid waste disposal is carried out negligently and without proper understanding of the nature of these materials. Therefore, the purpose of this study is to investigate the mechanical property of marine based biomaterial from squid gladius found along the Kenyan Coast. It is hoped that the results will shed light on potential applications of the biomaterials for bio-batteries, biosensor devices and biomedical applications and hopefully mitigate environmental pollution and degradation in Kilifi County.

The recent surge in interest in bioelectronics and the drive towards cheap, biocompatible and biodegradable components has increased the search for materials from natural, widely available and sustainable sources. Therefore, exact determination of the physicochemical properties of biomaterials is a subject of utmost importance for providing eco-friendly alternative materials for industrial applications. Squid gladius are readily available as a waste material from the local fish industry along the Kenyan Coast.

## 2. Theoretical Framework

### 2.1 Dynamic Mechanical Analysis(DMA)

Dynamic Mechanical Analysis is a technique that is widely used to characterize a material's properties as a function of temperature, time, frequency, stress, atmosphere or a combination of these parameters. DMA is a very popular and powerful technique that measures the transitions in materials because it is sensitive to side chain or main chain motions and local models in polymers. It characterizes the mechanical responses of materials by monitoring property changes with respect to temperature and/or frequency of oscillation. The technique separates the dynamic response of materials into two distinct parts: an elastic part (E') and a viscous damping component (E''). Specifically, in DMA a variable sinusoidal strain ( $\epsilon$ ) or stress ( $\sigma$ ) is applied to a sample and the resultant sinusoidal stress or strain is measured. If the material being evaluated is purely elastic, the phase difference between the stress and strain is zero (i.e. stress and strain are in phase). The stress  $\sigma$  and the deformation (strain)  $\epsilon$ ; are related through the Young Modulus E as follows:

$$\sigma = E\epsilon \quad (1)$$

The modulus is often known as the rigidity and is a quantity that is a representative of the materials resistance to deformation. Its reciprocal is the compliance J given by;

$$J = \frac{1}{\sigma} = \frac{1}{E\epsilon} \quad (2)$$

If a material is purely viscous, the phase difference is 90°. However, most real-world materials including

polymers are viscoelastic, both behave as elastic (Hookean) solid and viscous (Newtonian) liquid, such materials exhibit a phase difference between the extremes. This phase difference, together with the amplitudes of the stress and strain waves, is used to determine a variety of fundamental material parameters, including storage and loss modulus, loss factor ( $\tan \delta$ ), complex and dynamic viscosity, storage and loss compliance, transition temperatures, creep, and stress relaxation as well as related performance attributes such as rate of degree of cure, sound absorption impact resistance, and morphology.

Dynamic mechanical analysis measures the viscoelastic properties using either transient or dynamic oscillatory tests. Transient tests include creep and stress relaxation. In a creep relaxation, a stress is applied on a sample and held constant while the deformation is measured versus time. After a short time, the stress is removed and the recovery is measured as a function of time. In a stress relaxation, a deformation is applied to the sample and held constant, and the degradation of the stress required in maintaining the deformation is measured as a function of time. The sample is then released to an unstressed state, and its recovery is measured as a function of time. The dynamic oscillatory test is the most common, where a sinusoidal stress (or strain) is applied to a material and the resultant sinusoidal strain (or stress) is measured. Most DMA measurements are made using a single frequency and constant deformation (strain) amplitude while varying temperature.

## 2.2 Dynamic Mechanical Measurement

An alternative experimental procedure to creep and stress relaxation is to subject the specimen to an alternating strain and simultaneously measure the stress. For linear viscoelastic behavior, when the equilibrium is reached, the stress and strain varies sinusoidal, but the strain lags behind the stress. If stress  $\sigma(t)$  is applied, then altered with time  $t$ , and angular frequency  $\omega$ , the governing equation is:

$$\sigma(t) = \sigma_o \sin \omega t \quad (3)$$

where  $\sigma_o$  is the amplitude,  $\sigma$  is the stress,  $\omega$  is the angular frequency and  $t$  is the time. An ideal elastic body deformation instantly follows an applied stress, defined by;

$$\varepsilon(t) = \varepsilon_o \sin \omega t \quad (4)$$

where  $\varepsilon_o$  is the amplitude.

Polymers are not ideal elastic bodies; they are viscoelastic materials. In such cases the deformation (strain) lags behind the applied stress as shown in Figure 2. With ideal viscoelastic bodies, the resulting phase angle  $\delta$  in the corresponding vector diagram can be assumed to be constant, such that the deformation follows the above equation while the stress is given by:

$$\sigma(t) = \sigma_o \sin(\omega t + \delta) \quad (5)$$

where  $\delta$  is the phase angle,  $\sigma_o$  is the amplitude,  $\omega$  is the angular frequency and  $t$  is the time. The stress vector can be considered to be the sum of two components.

$$\begin{aligned} \sigma' &= \sigma_o \cos \delta \\ \sigma'' &= \sigma_o \sin \delta \end{aligned} \quad (6)$$

the first is in phase with the deformation while the second component is out of phase. A modulus can be assigned to each of the components.

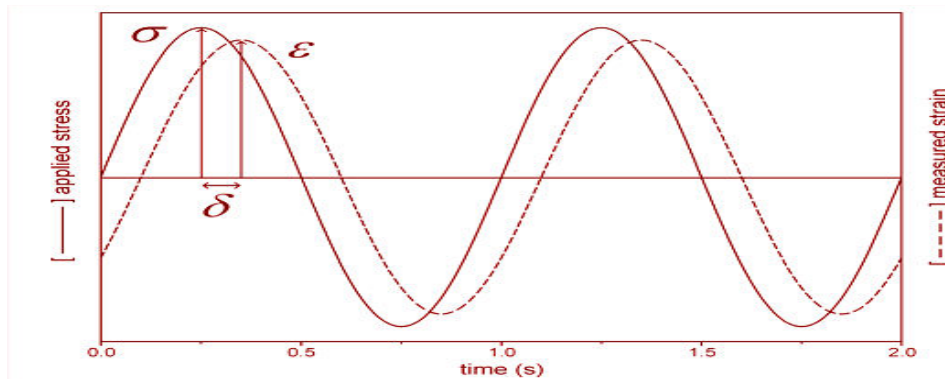


Figure 2: Stress and strain as a function of time with dynamic loading (Ward and Hadley, 1993).

The real modulus, or storage modulus,  $E'$ , measures the rigidity and resistance to deformation of the sample. It is related to the complex modulus of rigidity  $E^*$  by:

$$E' = \frac{\sigma'}{\epsilon_o} = \frac{\sigma_o}{\epsilon_o} \cos \delta = E^* \cos \delta \quad (7)$$

The imaginary, or loss modulus,  $E''$ , on the other hand, reflects the loss of useful mechanical energy through dissipation as heat;

$$E'' = \frac{\sigma''}{\epsilon_o} = \frac{\sigma_o}{\epsilon_o} \sin \delta = E^* \sin \delta \quad (8)$$

Similarly,  $E''$  is given by:

$$\log \frac{\alpha(T)}{\alpha(T_g)} = - \frac{C_1(T - T_g)}{C_2 + T - T_g} \quad (9)$$

The loss factor spectra can be quantitatively described by a superposition of model function [9];

$$E''(T) = \sum_{i=1}^2 A_i \exp \left\{ \frac{-E_i}{kT} \left[ \frac{1}{T^2} \left( \frac{1}{T_{m_i}} - \frac{1}{T} \right) \right] \right\} \quad (10)$$

In this model function  $A$  is a constant,  $k$  is the Boltzmann constant,  $T$  is the absolute temperature,  $T_m$  temperature representing maximum loss modulus,  $E$  is the activation energy and  $i$  refers to different processes which contribute to the mechanical response. Introducing the complex variables, one may express the strain  $\epsilon$ ; and stress  $\sigma$  as follows:

$$\epsilon^* = \epsilon_o e^{i\omega t} \quad (11)$$

The complex modulus  $E^*$  maybe then expressed as;

$$\sigma^* = \sigma_o e^{i(\omega t + \delta)} \quad (12)$$

where:  $i^2 = -1$ . Instead of following the deformation (strain) produced by a given stress, the sample can be strained and the resulting stress can be measured. The complex compliance defined as;

$$J^* = \frac{1}{E^*} \quad (13)$$

is obtained in this case and the storage and loss compliance are correspondingly given by:

$$E' = \frac{J'}{J'^2 + J''^2} \tag{14}$$

$$E'' = \frac{J''}{J'^2 + J''^2}$$

The complex dynamic shear modulus at frequency  $\omega$ ,  $E^*(\omega)$  expressed in pascal, is given by the ratio between the magnitude of the dynamic shear stress,  $\tau(\omega)$ , and the magnitude of the applied dynamic shear strain,  $\epsilon(\omega)$  as depicted in the following equation:

$$E^*(\omega) = \frac{\tau(\omega)}{\epsilon(\omega)} \tag{15}$$

The loss factor, storage modulus and loss modulus vary with frequency of loading as shown in Figure 3 below. At low frequency the polymer is rubber like and has a low storage modulus, which is independent of frequency. At high frequency, the polymer is glassy and the storage modulus is again independent of frequency. In the intermediate region where the material behaves viscoelastically, the storage modulus increases with increasing frequency. As the frequency is increased it becomes more difficult for the chains to respond to the applied forces and tend to remain in a frozen state. A frozen system stores more energy than a free system [10].

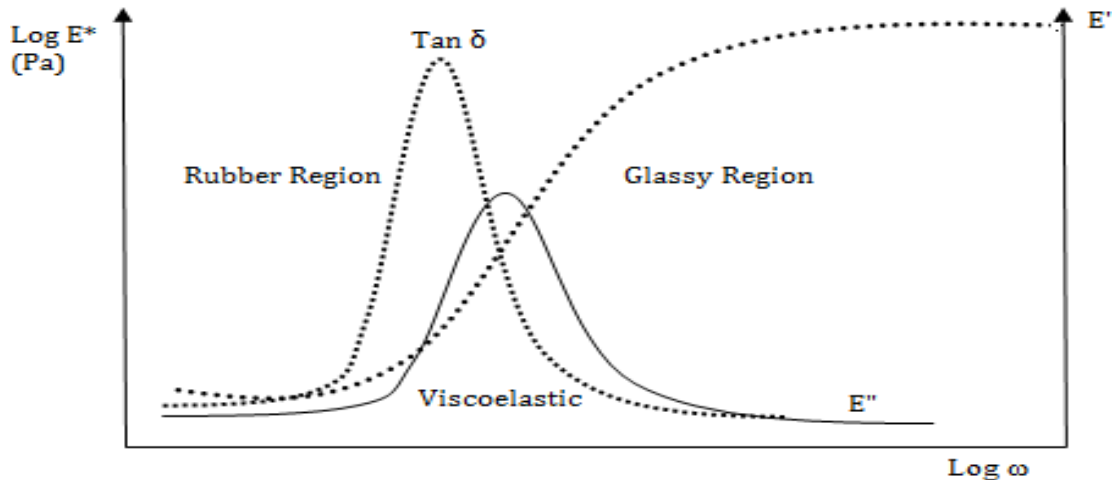


**Figure 3: The complex modulus,  $E^* = E' + iE''$ , as a function of frequency**

The loss modulus is zero both at low and at high frequencies where stress and strain are in phase for the rubbery and glassy phases. In the intermediate viscoelastic region, the loss modulus increases to a maximum value then decreases. If the mechanical force applied has a low frequency compared to the transition rates in the system, establishment of a thermal equilibrium is rapid and the system can always remain in equilibrium, hence we encounter quasistatic conditions and observe the full relaxation strength.

On the other hand when the frequency of the applied force is large compared to the transition rates, equilibrium cannot be established and the system reacts to the average strain only, which is zero. Crossover from one regime to the other occurs at  $\omega\tau \approx 1$  [10]. The phase angle, expressed as its sine or tangent, is an important parameter for describing the viscoelastic properties of a paving material. The complex, storage and loss moduli, and the phase angle are illustrated by the trigonometry of a right triangle, as shown in Figure 4

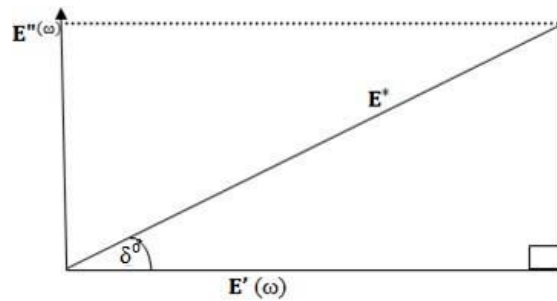


**Figure 4: Right angled trigonometric relation among the moduli  $E^*$ ,  $E'$ ,  $E''$  and the phase angle  $\delta$**

It follows that the loss tangent can be calculated simply as the tangent of the phase angle, or alternatively, as the ratio of the loss to storage moduli:

$$\tan \delta = \frac{E''}{E'} = \frac{1}{\omega \tau} \quad (16)$$

and that

$$E^* = \sqrt{E'^2 + E''^2} \quad (17)$$

where  $E^*$ , is the ratio of the peak stress to the peak strain, and reflects the total stiffness. The in-phase component of  $E^*$ , that is, the shear storage modulus,  $E'$ , represents the part of the input energy which is stored (the elastic portion). The out-of-phase component of  $E^*$ , that is, the shear loss modulus  $E''$ , represents viscous component of it. The complex dynamic shear viscosity  $\eta^*$  can be obtained from  $E^*$  divided by the frequency, while the dynamic viscosity is;

$$\eta = \frac{E''}{\omega} \quad (18)$$

### 2.3 DMA Measurement System

The DMA 2980 dynamic mechanical analyzer (TA instrument) incorporates a noncontact direct drive motor to deliver reproducible forces (stresses) over a wide dynamic range of 0.001 -18 N; an air bearing shaft support and guidance system to provide frictionless continuous travel over 25 mm from evaluating polymers at large oscillating amplitude ( $\pm 0.5 - 10,000 \mu\text{m}$ ); and optical encoder displacement sensor to provide high resolution of oscillation amplitude, which results in excellent modulus precision and  $\tan \delta$  sensitivity (0.0001); and a bifilar - wound furnace complemented by a gas cooling accessory to allow a broad temperature range ( $-150^\circ\text{C} \rightarrow 600^\circ\text{C}$ ) to be covered. The DMA 2980 (Figure 2.4) also features a variety of damping configuration to accommodate rigid bars, fibers, thin films and viscous liquids in bending, compression, shear, and tension modes of deformation.



**Figure 4: Dynamic mechanical analyzer model 2980**

### 3. Experimental Methods and Procedure

#### 3.1 Sample Collection and Extraction of Chitosan

Samples of squid gladii (SG) were collected from the coastal areas of Kenya. They were chosen specifically because of their abundant supply of marine wastes and also due to their contrasting environmental conditions and geographical locations. The extraction process is summarized in the block diagram below (Figure 6) and involves the following processes;

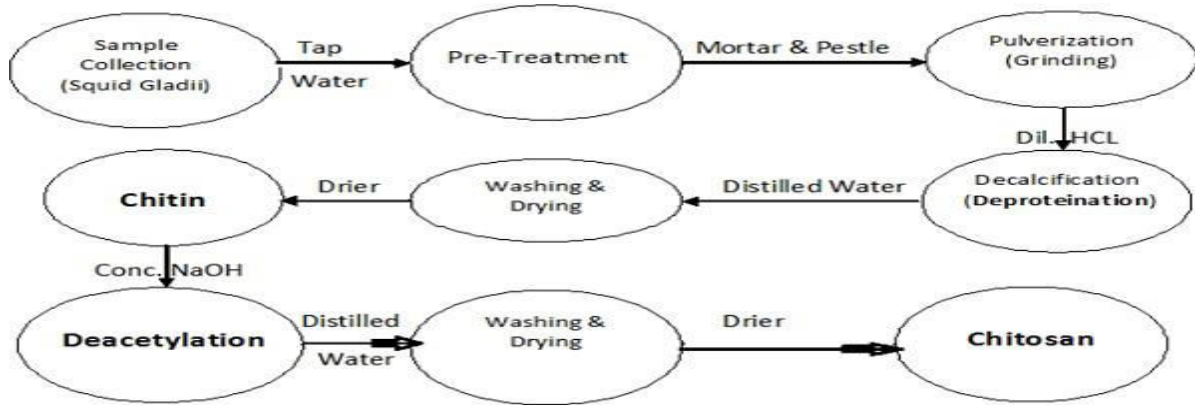


**Figure 6: Summary of the process of chitosan extraction**

The SG samples collected were washed with water and then soaked in a mild sodium hydroxide solution, (1% w/v NaOH) to remove non-chitin rich organic material. This was followed by washing and air drying at room temperature for two days. The dry SG were then pulverized into powder using a mortar and pestle and then sieved with a 1.5mm sieve. Demineralization was done by putting the SGP in mild hydrochloric acid solution (1 M HCl at a ratio of 1:10 w/v) for 2 hours. This was followed by filtering and washing with distilled water. The deproteination step was done by putting the demineralized SGP in a mild sodium hydroxide solution of 5% w/v NaOH at 70° C at a ratio of 1:10 w/v overnight. The resulting chitin was filtered and washed with distilled water until neutral pH then dried in a hot air oven at 60° C for six hours and then weighed. The dry chitin powder obtained was refluxed in concentrated sodium hydroxide solution of 50% NaOH at a temperature of 100°C for six hours in the ratio 1:10 w/v. The resulting chitosan was washed thoroughly with distilled water until neutral pH and dried in hot air oven at 60°C for 8 hours and then weighed. The dry CP was then stored in a desiccator.

Two different Chitosan film samples were made. The first one (sample A) of 0.5% concentration and other (sample B) of 1% from which Chitosan films were made by the solution casting method.

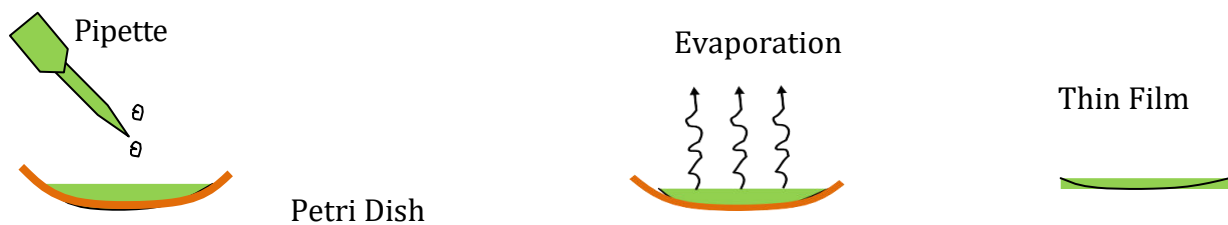


**Figure 7: Solution casting method**

Some other chitosan films (sample C) were prepared by the drop casting method. In this method,

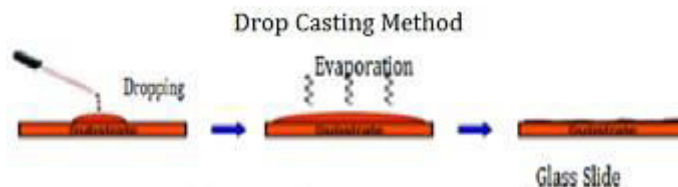


**Figure 8: Drop casting Method showing the steps in preparing chitosan thin films**

### 3.3 DMA Sample Characterization

Dynamic mechanical measurements were employed to investigate relaxation events and also to the study of the viscoelastic response of the chitosan film samples. Kinetic parameters such as activation energy, pre-exponential factor and reaction order, give a quantitative measure of thermal stability of a material. Normally at a lower temperature, other relaxation processes can be observed for polymeric materials. The  $\beta$  relaxation is normally attributed to polymer backbone conformation reorganization. The DMA equipment (TA instruments DMA 2980) was calibrated according to the manufacturers' recommended procedures. DMA measurements were conducted at a heating rate of 5 °C/min, testing temperature ranging from 25-200 °C and a frequency of 1 Hz. The dimensions of the testing sample were; thickness 0.07 mm, width 9.44 mm and length

15.21 mm. The loss and storage moduli were recorded in a DMA multi-frequency single cantilever mode system. The storage and loss moduli were measured in the frequency range 0.1-30 Hz. The temperature range was from 298 to 375 K in steps of 2 K after every frequency sweep. The sample was clamped as shown in Figure 9. It took about 120 minutes to run a measurement.

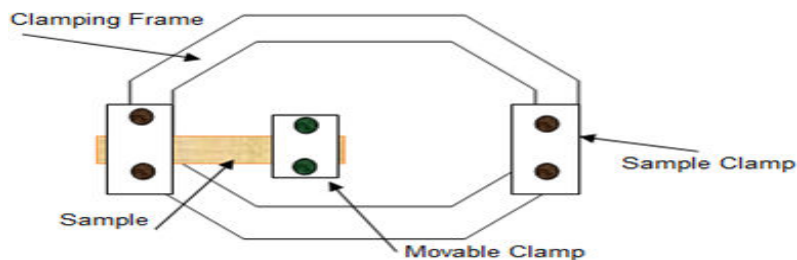


**Figure 9: Front view of a single cantilever showing the sample position and the movable clamp**

## 4. Results and Discussion

### 4.1 Effects of temperature, concentration and frequency on the relaxation processes

To observe the effects of factors on relaxation processes, graphs of storage modulus, loss modulus and loss factor against temperature at various frequencies and concentration were plotted as shown below.

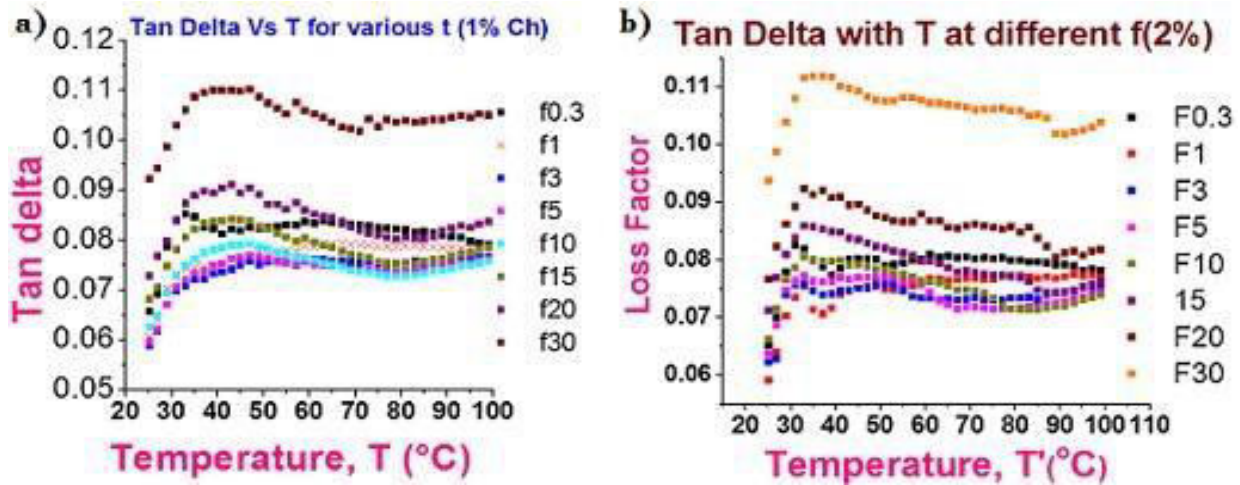


Figure 10: Effects of Temperature, Concentration and frequency on the relaxation processes

From Figures 10a and 10b, we see the first transition marked by tan delta peaks for the films ranging between 30°C - 50°C which generally seem to increase with frequency and chitosan concentration. This is the  $\beta$ -relaxation which normally occurs at a lower temperature and is assigned to the local side-chain movement of the polymer. This is in agreement with values obtained in literature. Chitosan films exhibit two  $\tan \delta$  peaks at positions around 30 – 50°C. According to Mucha and Pawlak [12], those peaks are attributed to relaxation processes.

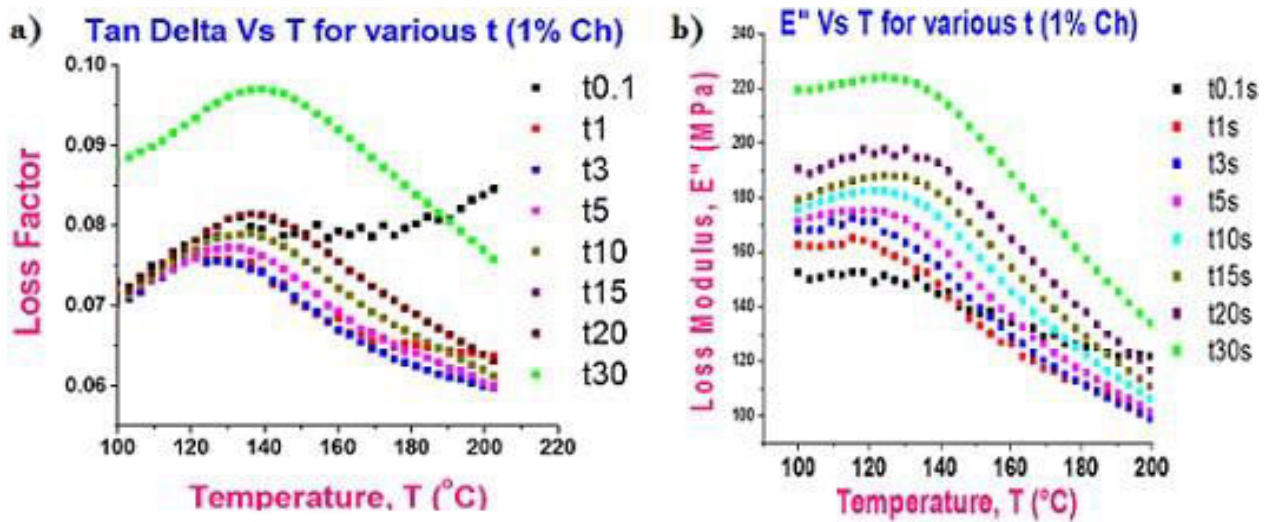
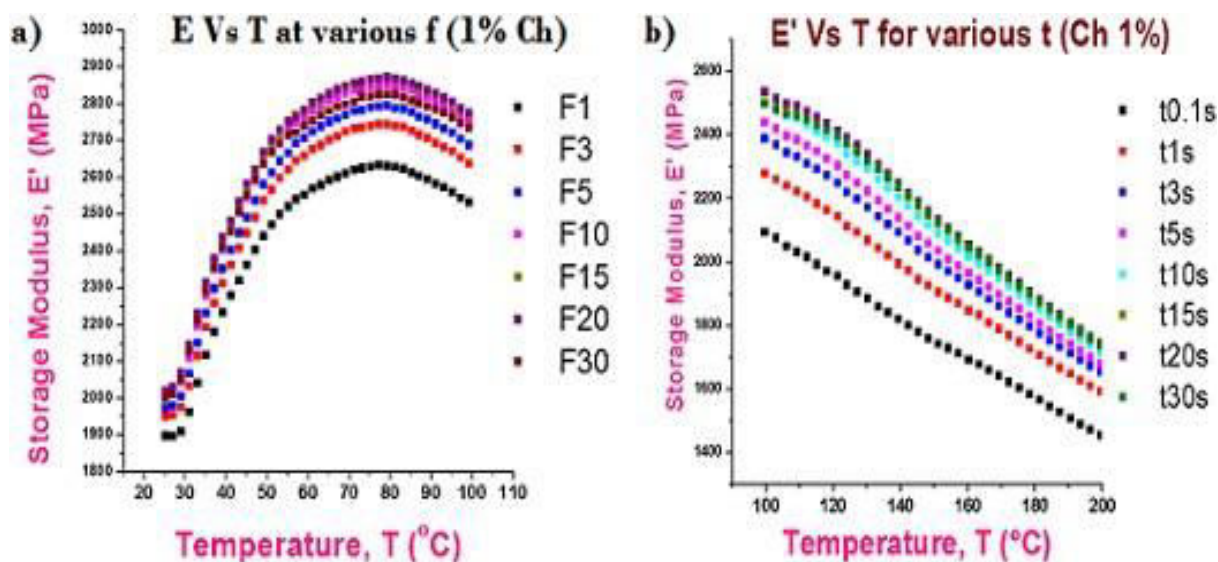


Figure 11: Graphs showing the variations (a) of Loss factor and (b) Loss modulus with temperature for different loading times for Ch

Another transition can be seen in Figure 11a between 125-150°C which is the glass transition ( $T_g$ ) which also shifts with frequency. This is confirmed by the peak of the loss modulus plot in Figure 11b. The figure shows that  $\alpha$ -process (loss modulus peaks) shifts to higher temperature with increasing frequency and this indicates a true relaxation process. This shift can be attributed to the fact that at low frequency, almost all the chains are able to follow movement of the oscillations.

At higher frequency however, it becomes very difficult for all the chains to follow the movement of the oscillations. This can be explained by the fact that when the timescale of molecular motion coincides with that of mechanical deformation, each oscillation is converted into the maximum- possible internal friction and nonelastic deformation. The loss modulus, which is a measure of this dissipated energy, also reaches a maximum.



**Figure 12: Graphs showing the variation of Storage modulus with temperature for various frequencies and loading time for Chitosan**

Toffey and Glasser [13] noticed  $\alpha$  -relaxation between 60 and 94 $^{\circ}\text{C}$  for ionic complexes of chitosan. The temperatures of relaxations increase for amidized chitosan derivatives [13]. There are some ranges of  $T_g$  values reported by other researches mainly due to the difference in sample and instrumental methods. For example, the  $T_g$  of chitosan is reported to be about 150 $^{\circ}\text{C}$  by Kakizaki et al 1988 and 141.2 $^{\circ}\text{C}$  by Nelly et al, 2005. Ratto et al [14] reported glass transition temperature at 30 $^{\circ}\text{C}$ , Lazaridou and Biliaderis 2002 found  $T_g$  ranging from -23 $^{\circ}$ - 67 $^{\circ}\text{C}$  as per the water content in them. This indicates plasticizing effect of water in both the above cases. Whereas Sakurai [15] reported  $T_g$  of chitosan at 203 $^{\circ}\text{C}$ . Two other transitions were observed at 280 and 321 $^{\circ}\text{C}$  associated with a partial and total decomposition of the chitosan. Thus knowing the temperature at which the two transitions occur can give us an insight of operating temperature range of the biomaterial, in this case our material has an operation temperature range of 50 $^{\circ}\text{C}$  - 120 $^{\circ}\text{C}$ .

Figure 12 shows plots of the storage modulus against temperature for different frequencies of the samples. The storage modulus decreased gradually with temperature which shows that a transition takes place within the 120 - 200 temperature range. The value of  $E'$  tends to increase with frequency which is attributed to the lesser mobility of polymeric chains at higher frequency. That is, as frequency is increased it becomes difficult for the chain to respond to the applied forces and tend to remain in a frozen state. A frozen system stores more energy than a free system. It is observed that storage modulus of the material decreases with increasing temperature which is related to the increase in viscosity and polymer chain mobility of the matrix at higher temperatures.

#### 4.2 Time-Temperature Dependence of Relaxation Time

The activation energy  $E_a$  was determined by performing an Arrhenius plot of the data where the natural log of frequency was plotted against temperature as shown in figure 13 below.

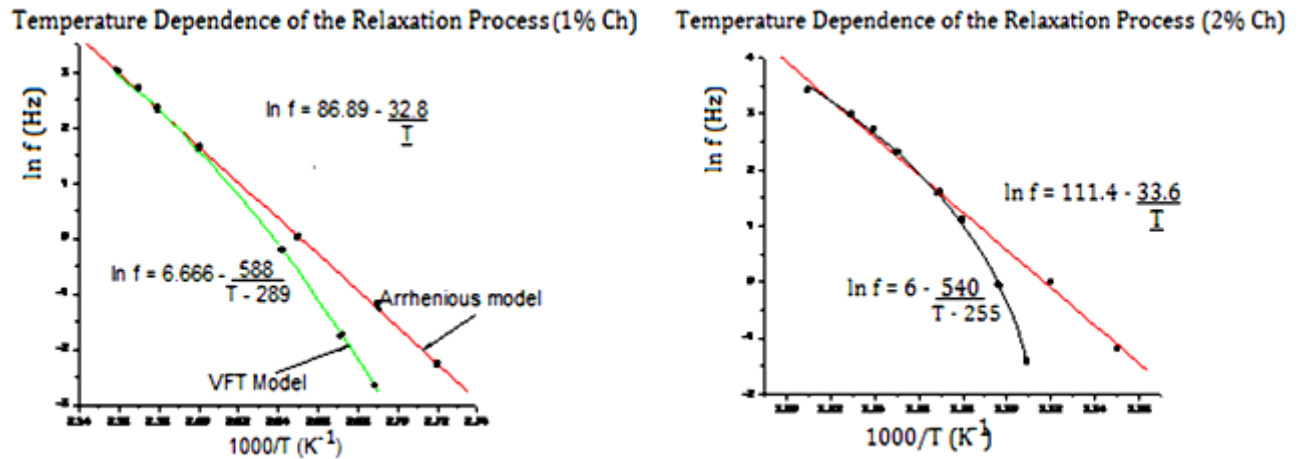


Figure 13: Temperature dependence of the relaxation processes (a)1% Ch and (b)2% Ch

The time-temperature dependence of mean relaxation time for the films follows the Arrhenius law [equation 22] and VFT law [equation 19] as observed from figure 13 confirming that these are dynamic glass transition processes. The regression value,  $R^2$  of 0.99 implies that the plotted points can be said to lie in a straight line. The red lines have been fitted using the Arrhenius model while the green and black curves are fitted with the VFT model with the fit parameters given in table 1 below. In the VFT relation we have;

$$\tau = \tau_0 \exp\left[\frac{B}{T - T_0}\right] \quad (19)$$

Where  $\tau_0$  is the pre-exponent factor or the relaxation time in the absence of energy barrier. B is a constant; T is the absolute temperature and  $T_0$  is the ideal Vogel temperature which is 50°C below  $T_g$ . Since the relaxation time is inversely proportional to the frequency, we can have;

$$\ln f = \ln f_0 - \frac{B}{T - T_0} \quad (20)$$

In the Arrhenius relation we have;

$$f = f_0 \exp\left[-\frac{E_a}{RT}\right] \quad (21)$$

where  $f_0$  is the pre-exponential or frequency factor and  $E_a$  is the activation energy, R is the gas constant which is 8.314J/Mol.K and T is the temperature in Kelvin. This can also be written as;

$$\ln f = -\frac{E_a}{R} \left(\frac{1}{T}\right) + \ln f_0 \quad (22)$$

The Arrhenius plot of the logarithm of frequency against the reciprocal of temperature is shown in figures 13 which gave the fit parameters as shown in the table below.

Table 1: Fit parameters for the Arrhenius and VFT models for the 1% and 2% Chitosan samples

Parameter	Arrhenius Model		VFT Model	
	1% Ch	2% Ch	1% Ch	2% Ch
$f_0$	$5.44 \times 10^{37}$	$2.4 \times 10^{43}$	786	403
$E_a$	272.7KJ/Mol	279.4KJ/Mol		
B			588	540
$T_0$			289	255
$T_g$			239	205

To determine the viscoelastic properties, a plot of the storage modulus against the loss modulus was made (Figure 14). It gave a straight line graph whose slope gave the loss factor ( $\tan \delta$ ), which is a measure of the mechanical damping or internal friction of the material under a load. The phase angle also tells us whether a material is purely elastic, purely viscous or is viscoelastic.

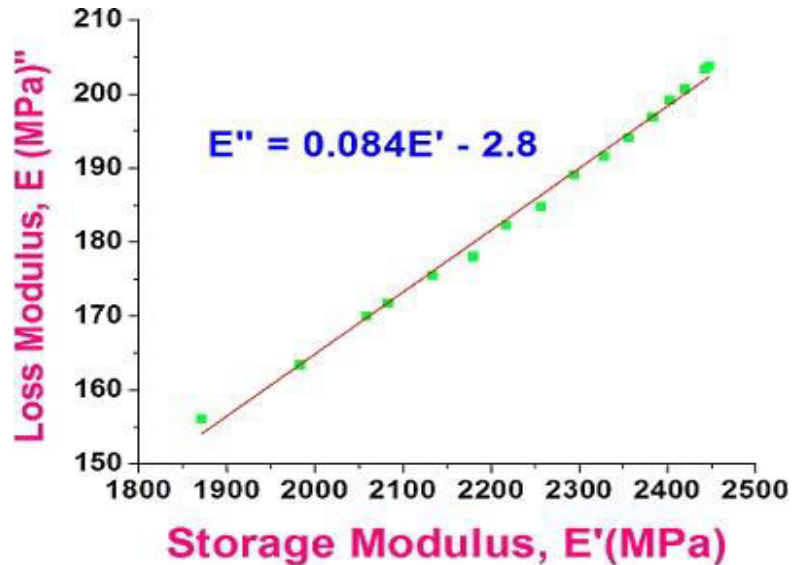


Figure 14: Graph showing the Loss modulus versus storage modulus

From Figure 14 we see a linear relationship between  $E''$  and  $E'$  giving the phase angle ( $\delta$ ) as  $4.8^\circ$  ( $\pi/38$ rad). The phase angle  $\delta$  is the phase difference between the dynamic stress and the dynamic strain in a material subjected to a sinusoidal oscillation. If the material being evaluated is purely elastic, the phase difference between the stress and strain is zero (i.e. stress and strain are in phase) while if a material is purely viscous, the phase difference is  $90^\circ$ . Thus, the material under investigation is viscoelastic (i.e. it both behaves as elastic (Hookean) solid and viscous (Newtonian) liquid, since it exhibits a phase difference between  $0 - 90^\circ$ ). The obtained value of the loss factor ( $\tan \delta$ ) = 0.084 shows that the material under study has very low mechanical damping which means its rigidity and resistance to deformation is very high.

## 5. Conclusions and Recommendations

This work presents the extraction and characterization of a marine based biomaterial from squid pens found along the Kenyan coast using DMA. DMA results showed that the material under investigation is viscoelastic with very low mechanical damping which means its rigidity and resistance to deformation is very high. The operation temperature range of  $50^\circ\text{C} - 120^\circ\text{C}$  and the  $E_a$  value of  $272.7\text{kJ/mol}$  of the biomaterial is ideal for its possible applications in biotechnological industries due to its product cost and environmental safety.

Further research to improve the material's properties especially opto-electric, mechanical and structural properties needs to be explored.

## Appendix

Photos showing the stages of the chitosan sample from the source to the final product



## References

1. C.K. Pillai, W. Paul, and C.P. Sharma. Chitin and chitosan polymers: Chemistry, solubility and fiber formation. *Prog. Polym. Sci.*,34(7):641 – 678,2009.
2. M. Ward and D. W. Hadley. An introduction to the mechanical properties of solid polymers, volume 334. Wiley, Chichester, UK,1993..
3. K.M. Rudall. The chitin/protein complexes of insect cuticles. In *Advances in Insect Physiology*, eds., volume 1. London :Academic, 1 edition,1963.
4. M. Mucha and A. Pawlak. Thermal analysis of chitosan and its blends. 427(1 - 2):69 – 76,2005.
5. Ackah Toffey and Wolfgang G. Glasser. Chitin derivatives iii formation of amidized homologs of chitosan.8(1):35 – 47, 2001.
6. J. Ratto and T. Hatakeyama. DSC investigation of phase transitions in water/chitosan system. 36:2915 –19,1995.
7. K. Sakurai, T. Maegawa, and T. Takashi. Glass transition temperature of chitosan and miscibility of chitosan/poly (n-vinyl pyrrolidone) blends. 41:7051 – 7056,2000.
8. T.H. Silva and A. Alves and B.M. Ferreira and J.M. Oliveira and L.L. Reys and R.J.F. Ferreira and R.A. Sousa and s.s. Silva and J.F. Mano and R.L. Reis (2012) Materials of marine origin: a review on polymers and ceramics of biomedical interest. *Int Mater Rev* 57:276–306(31).
9. Raushan Kumar Singh, Ye-Wang Zhang, Ngoc-Phuong-Thao Nguyen, Marimuthu Jeya, and Jung-Kul Lee. Covalent immobilization of  $\beta$ -1-4-glucosidase from *agaricus arvensis* onto functionalized silicon oxide nanoparticles. 89(2):337 – 344,2010.
10. M. A Meyers, Chen Po-Yu, A.Y. Lin, and Y. Seki. Biological materials: Structure and mechanical properties. *Progress in Materials Science*, 53:1 – 206,2008
11. G. Austin, A. J. Springthorpe, B. A. Smith, and C. E. Turner. Electronic transport phenomena in single-crystal nio and coo. *Proceedings of the Physical Society*, 90(1),1981.
12. R. A. A. Muzzarelli, (2011), Chitin nanostructures in living organisms, in N. S. Gupta (ed.) Chitin, volume 34, chapter 1, pp. 1–34, Springer, Netherlands, ISBN978-90-481-9684-5.
13. Domard, : A perspective on 30 years research on chitin and chitosan. *Carbohydrate Polymers* 2012, 84(2), 696- 703.
14. M. Rinaudo,; Chitin and chitosan: Properties and applications. *Progress in Polymer Science* 2006, (7),603-632.
15. S.K. O’Leary, S. R. Johnson, and P.K. Lim. The relationship between the distribution of electronic states and the optical absorption spectrum of an amorphous semiconductor: An empirical analysis. 82:3334,1997.